

## 44. A PROGRESS REPORT ON THE CARINA SPIRAL FEATURE

B. J. BOK, A. A. HINE, and E. W. MILLER

*Steward Observatory, Tucson, Ariz., U.S.A.*

**Abstract.** The existing data on the distribution of O and B stars, of optical and radio H II sources, of H I and of cosmic dust have been assembled for the Carina-Centaurus Section of the Milky Way,  $l^{II} = 265^\circ$  to  $305^\circ$ . The published data have been supplemented by recent photoelectric UBV data and new photographic material. Two Working Diagrams (Figures 9 and 10) of the Carina Spiral Feature have been prepared. The Feature is sharply bounded at  $l^{II} = 282^\circ$  and again at  $l^{II} = 295^\circ$  in the range of distance from 1.5 to 6 kpc from the sun. Its outer rim is observed from the sun almost tangentially to a distance of 8 kpc from the sun. The Feature is found to bend at distances greater than 9 to 10 kpc from the sun, a result shown by both radio H I and radio H II data.

Figure 9 presents our basic data for the stellar, gas and dust components of the Feature. The O and early B stars and the H II Regions are closely associated and within 6 kpc of the sun they are concentrated in the range  $285^\circ < l^{II} < 295^\circ$ . The distribution in longitude of H I is broader and spills over on both sides of the O and B and the H II peak distributions. Long period cepheids yield a concentration similar to that shown by O and B stars and H II Regions. The visual interstellar absorption between  $l^{II} = 282^\circ$  and  $295^\circ$  is represented by a value  $A_V = 0.5 \text{ mag kpc}^{-1}$ , or less, applicable to distances of 4 to 5 kpc. Much higher absorption is present on the outside of the Carina Spiral Feature,  $265^\circ < l^{II} < 280^\circ$ , where total visual absorptions as great as 3.5 mags. are found at distances of the order of 2 kpc. Even heavier absorption is indicated for these longitudes at 4 kpc from the sun, thus suggesting that the heavy obscuration on the outside of the Carina Spiral Feature is a phenomenon of general structural relevance (see Figures 8 and 9). Only small values of  $A_V$  are found at the inside of the Spiral Feature.

The Working Diagram (Figure 10) shows that the O and B star peak and the H II peak have a width of 800 parsecs ( $12^\circ$ ) at 4 kpc from the sun, whereas the H I width is at least 1500 parsecs at the same distance. The peak of the O and B star distribution and of the H II distribution lies at about 600 parsecs ( $8^\circ$  at 4 kpc) within the outer edge of the spiral feature. The heaviest interstellar absorption is on the outside of the Feature.

### 1. Preamble

In the early 1950s Baade and Mayall (1951) found from their studies of external galaxies that emission nebulae and O and early B stars are the best tracers of spiral arms. Morgan *et al.* (1952) accepted the challenge that these same objects should be used to trace the spiral structure of our Galaxy. Thus, the first diagrams of the local spiral structure were obtained. Their work was extended later by Becker and Fenkart (1963), Becker (1963, 1964) and by Schmidt-Kaler (1964). The presence of three local spiral features was suggested: the Perseus Arm, the Orion Arm, and the Sagittarius Arm. The Carina H II regions and OB stars were provisionally linked to the Sagittarius Arm, but they did not receive the attention they deserved. The pitch angle, the angle between the direction of an arm and the direction of rotation, for the three arms averaged about  $25^\circ$ .

The 21 cm line of neutral atomic hydrogen was discovered by Ewen and Purcell (1951) and the results of the first extensive studies of spiral structure based on 21 cm profiles by the Leiden and Sydney observers became available shortly after the publication of the Morgan-Sharpless-Osterbrock results. They revealed an overlying near-circular spiral pattern of H I distribution. The Leiden-Sydney hydrogen map by Oort *et al.* (1958), and more recently the studies by Westerhout (1968), Kerr

(1969b), and Hindman (1969), show the spiral arms to be circular, with pitch angles of only  $5^\circ$  to  $6^\circ$ . These pitch angles are much smaller than those found by Becker and Schmidt-Kaler.

To reconcile the optical and radio pictures of the Galaxy, Bok (1959) suggested that the Carina Spiral Feature is part of a spiral arm separate from the Sagittarius Arm, and that this feature extends possibly through the sun to connect with the Cygnus Arm. The Orion Arm is then considered to be a second-class spiral feature, a spiral spur rather than a spiral arm. Bok's emphasis on the Carina Feature goes back to his doctoral thesis (1932). The importance of the Carina Feature was stressed especially by him in 1937 in *The Distribution of the Stars in Space* (University of Chicago Press), notably in the concluding section of the book. A Carina-Cygnus spiral arm would possess a pitch angle in good agreement with the pitch angles found from 21 cm studies.

Recent investigations in Carina have strengthened the importance of the concentrations of OB stars and interstellar gas in Carina as a major spiral feature. Becker (1956) and Bok (1956) have stressed the high concentration of O and B stars in Carina

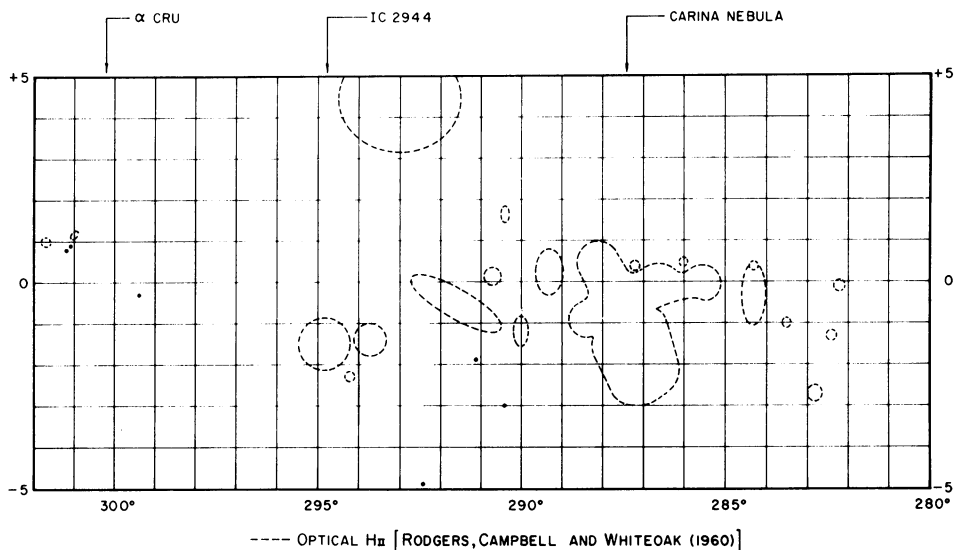


Fig. 1. The distribution of optical H II regions in Carina. Dotted lines indicate the optical H II regions in the list of Rodgers, *et al.* (1960a). The coordinates are  $l^{II}$ ,  $b^{II}$ . The positions of the three optically bright objects are indicated: the Carina Nebula, IC 2944, and the first magnitude binary star  $\alpha$  Crucis. In order to show the apparent H II distribution schematically, dimensions of the regions (as given by Rodgers *et al.* (1960a)) are used as the axes of the ellipses. Relative brightnesses are not shown. *The Mt. Stromlo H-Alpha Emission Atlas* (Rodgers *et al.* 1960b) was consulted for confirmation of the position, orientation, and shape of each object. Since the outline of RCW 54 (a large emission region between  $l^{II} = 289^\circ$  and  $291^\circ$ ) could not be ascertained, the four concentrations within the region, given in the notes to Tables II and III of Rodgers *et al.* (1960a) are shown in the figure. Many optical H II regions appear in the longitude range  $l^{II} = 282^\circ$  to  $295^\circ$ ; there are very few H II regions outside these limits. Note also that the H II regions appear generally south of the galactic plane. The single large H II region north of  $b^{II} = 0^\circ$  is RCW 59, which is probably a nearby object because of its relatively high galactic latitude ( $+4.5^\circ$ ) and its radial velocity ( $-12.2 \text{ km s}^{-1}$ ) as observed by Courtès (1969); its probable distance is 1.7 kpc.

with distances ranging from 1 to 4 kpc. More recent observations by Feinstein (1969) have revealed the presence of OB stars to distances of 6 kpc and Graham (1970) has observed OB stars in Carina to distances of 8–10 kpc. Extensive H II catalogues by Hoffleit (1953) and by Rodgers *et al.* (1960a) show the Carina region to be abundant in emission nebulae.

Radio studies of H II are providing additional valuable information. The continuum studies of Mathewson *et al.* (1962) and of Hill (1968) have revealed the presence of many thermal H II regions in the Carina-Centaurus section. There have been studies recently by Wilson (1969) by the newly-developed hydrogen 109  $\alpha$  techniques. Radial velocities have been obtained for most H II regions in this section. From these radial velocities, kinematical distances are found for many optical H II regions and also for H II regions which are too distant to be observed optically. The Wilson results clearly show that we are looking tangentially along a spiral feature to distances of 8–9 kpc and that the feature curves at distances of 9–10 kpc. Further support for the presence of a major Carina Spiral Feature is provided by the long-period cepheids. In the most recent paper on the subject, Fernie (1968) has found that the cepheids near  $l^{\text{II}} = 280^\circ$  to  $290^\circ$  extend to distances of 10 kpc; the Carina Feature is shown beautifully in his Figure 2.

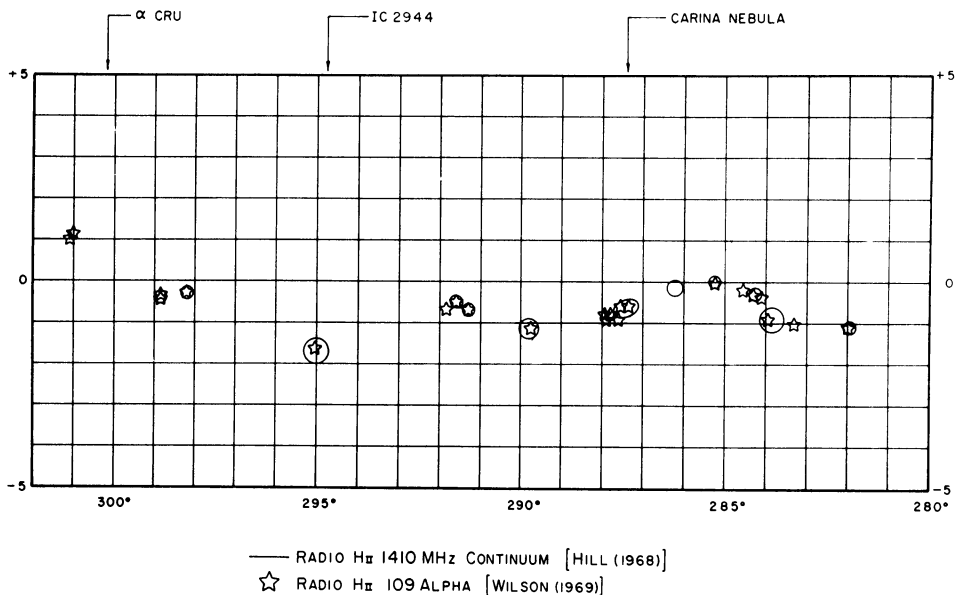


Fig. 2. The distribution of radio H II sources in Carina. Solid lines indicate schematically the 1410 MHz continuum sources observed by Hill (1968). Stars mark the positions of the H II 109 $\alpha$  line observations of Wilson (1969). Sources which have been found to be nonthermal by Mathewson *et al.* (1962) or by Wilson (1969) are not shown. For the continuum sources, the positions and the dimensions at half intensity are taken from Hill's contour map and are necessarily approximate. Relative brightnesses are not shown. The radio H II sources, like the optical sources, are concentrated in Carina between  $l^{\text{II}} = 282^\circ$  and  $295^\circ$  and south of the galactic plane. The two sources between  $298^\circ$  and  $299^\circ$  are very distant, and hence are not part of the nearer concentration between  $282^\circ$  and  $295^\circ$ ; they are discussed in the caption for Figure 3.

Because of the volume of evidence pointing to a major spiral feature in Carina which runs to great distances along the line of sight, we have undertaken a study in Carina of the distribution of OB stars, emission nebulae, H I and cosmic dust as a function of galactic longitude. Such a study should enable us to make cross cuts through the spiral feature at various distances and thus determine where the OB stars, emission nebulae, H I and dust are located. This paper is a progress report on our work to date.

The results are shown in terms of 9 figures each with a lengthy descriptive caption. We have brought together in one place all the data accessible to us in print, or made available to us in advance of publication. B. J. Bok and P. F. Bok are publishing their standard sequences and UBV magnitudes and colors for individual OB stars in a separate paper (Bok and Bok, 1969), but the derived absorptions are given in the figures that follow. A section entitled Conclusions and Recommendations will be found at the end of the Progress Report.

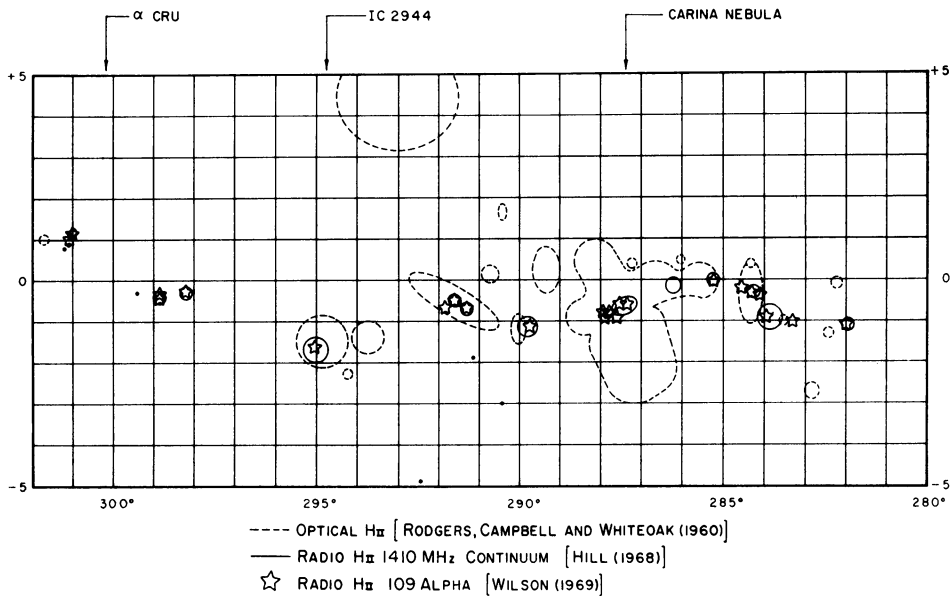


Fig. 3. Optical and radio H II. The optical and radio H II distributions of Figures 1 and 2 are here combined. Most of the radio sources correspond to optical H II regions. The sources observed between  $l_{II} = 298^\circ$  and  $299^\circ$  have no optical counterparts, but this is not surprising, since their kinematical distances from H II 109 $\alpha$  data are of the order of 11–12 kpc. At this distance the Carina Spiral Feature has bent over, and we are no longer viewing the feature tangentially. An analysis of the combined radio and optical data permits us to place a boundary on the Carina Spiral Feature. If we exclude the distant sources between  $l_{II} = 298^\circ$  and  $299^\circ$ , we find in the figure a region of low H II concentration between  $l_{II} = 295^\circ$  and  $302^\circ$ . Hill's work at 1410 MHz (1968) shows that this gap extends to  $l_{II} = 305^\circ$ . This lack of emission nebulae strongly suggests an interarm direction. For the other side of the Carina Spiral Feature the Mathewson *et al.* (1962) 1440 MHz observations show no H II sources between  $l_{II} = 265^\circ$  and  $282^\circ$ , again suggesting an inter-arm direction. We place the boundaries of the Carina Spiral Feature between  $l_{II} = 282^\circ$  and  $295^\circ$  for distances up to 10 kpc from the sun.

Beyond 10 kpc the feature is no longer observed tangentially.

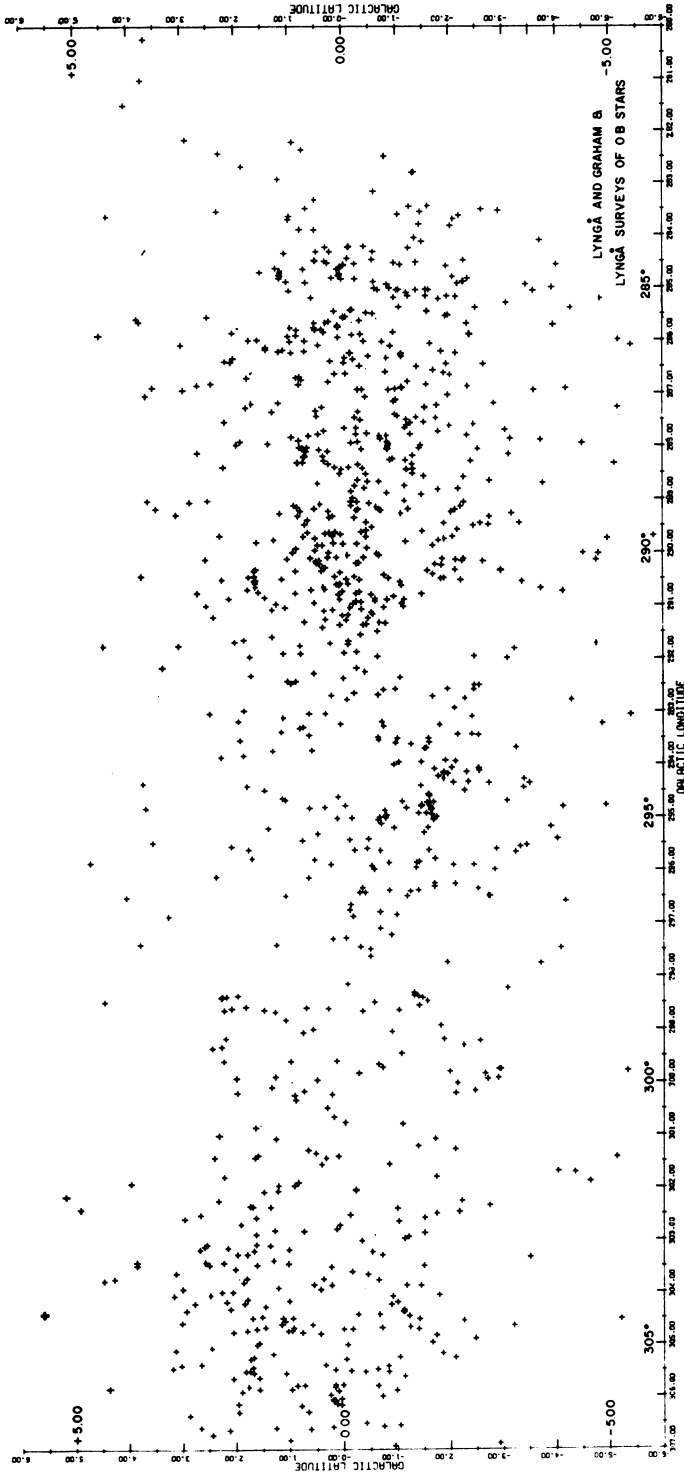


Fig. 4. Graham-Lyngå (1965) OB stars, Lyngå Carina-Centaurus (1968a) OB stars and Klare and Szeidl OB stars between  $l^{\text{II}} = 280^\circ$  and  $307^\circ$ . Three extensive Catalogs of OB stars have been used in the preparation of Figure 4, which shows the distribution over the sky of known OB stars to a limiting apparent magnitude between 11 and 12. We draw attention to the following features: (1) The concentration of OB stars is greatest between  $l^{\text{II}} = 284.5^\circ$  and  $l^{\text{II}} = 291^\circ$ . (2) There is a marked secondary concentration near IC 2944, at  $l^{\text{II}} = 295^\circ$ ,  $b^{\text{II}} = -1^\circ.5$ . (3) There is evidence for the presence of an obscuring cloud near  $l^{\text{II}} = 292^\circ$ ,  $b^{\text{II}} = -1^\circ.5$ . (4) Some faint OB stars make an appearance at positive galactic latitudes near  $l^{\text{II}} = 296^\circ$ , but the numbers at comparable negative galactic latitudes are still much larger than those at positive latitudes. The computer card catalog used in the preparation of Figure 4 was copied for us by Westerlund from an unpublished catalog compiled by Lyngå.

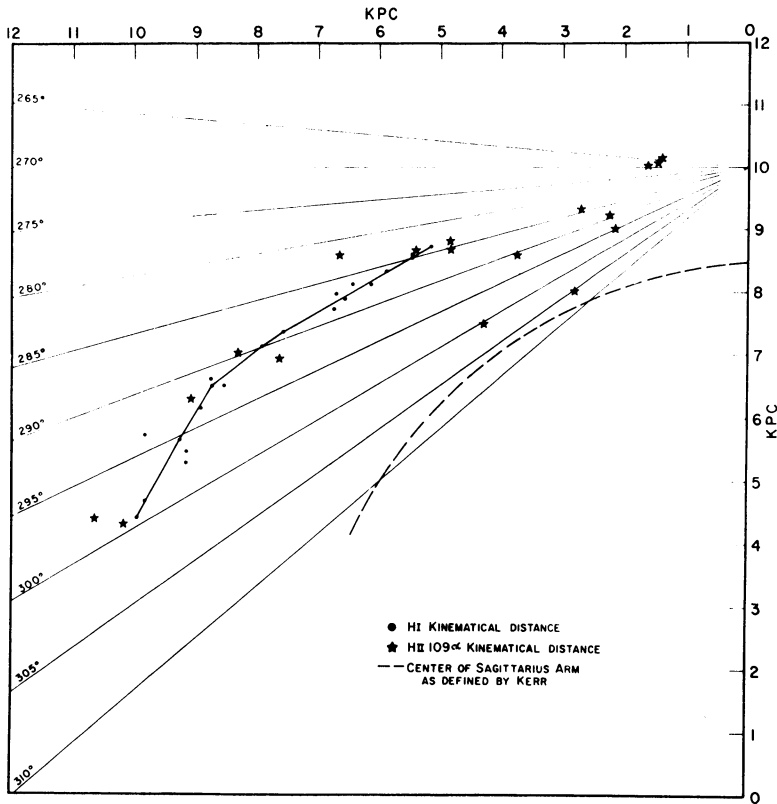


Fig. 5. The spatial distribution of H I and H II 109 $\alpha$  sources in Carina. To obtain the kinematical distances of the H I and the H II 109 $\alpha$  sources, the Schmidt model of the Galaxy was used (Schmidt, 1965). Kerr and Hindman (1969) provided the H I velocity profiles and Wilson (1969) provided the radial velocities for the 109 $\alpha$  sources. Because of the poor distance resolution between  $l^{\text{II}} = 270^\circ$  and  $295^\circ$  and because of the double-valued distances obtained inside the solar circle, the radio H I data have not been used to define the Carina Spiral Feature within 5 kpc of the sun. At distances greater than 5 kpc, the radial velocities resulting from galactic rotation are all greater than zero and the observed radial velocities yield unique distances. The dots in the diagram represent the kinematical distances of the neutral hydrogen beyond 5 kpc. A solid line has been drawn to connect the dots and defines the spiral feature as determined from the H I. Because of deviations from circular motion of  $\pm 10 \text{ km s}^{-1}$  a distance error of 1 kpc may result. The stars represent the kinematical distances of the H II 109 $\alpha$  sources. At distances greater than 5 kpc from the sun the H II 109 $\alpha$  sources agree well with the H I positions and strengthen the manner in which we have drawn the spiral feature. At distances less than 5 kpc from the sun, where double valued distances are derived, the radio H II 109 $\alpha$  sources can be identified with optical H II sources from position correspondence. Whenever this is the case, that kinematical distance of the radio source is chosen which best agrees with the optical distance of the observed H II region. No radio H II 109 $\alpha$  sources are observed between  $l^{\text{II}} = 270^\circ$  and  $282^\circ$ . The source at  $l^{\text{II}} = 282^\circ$  has a kinematical distance of 7 kpc and lies near the faint Rodgers *et al.* (1960a) optical source RCW 46. The position correspondence is not exact, and we may be looking at a close optical source near  $l^{\text{II}} = 282^\circ$  in front of a more distant source at 7 kpc from the sun. Optical counterparts to the H II 109 $\alpha$  sources are observed between  $l^{\text{II}} = 285^\circ$  and  $295^\circ$  with some near and some very distant sources superimposed near  $l^{\text{II}} = 290^\circ$ – $291^\circ$ . Beyond  $l^{\text{II}} = 295^\circ$ , however, no large optical H II regions are observed. At  $l^{\text{II}} = 298^\circ$  a very distant radio H II region is observed at 11–12 kpc distance from the sun (see Figure 3). At  $l^{\text{II}} = 301^\circ$  a visible H II region is observed which corresponds to an H II 109 $\alpha$  source. It is small and we will neglect it as insignificant; it corresponds to RCW 65. At  $l^{\text{II}} = 305^\circ$  a strong optical H II region is observed which corresponds to a strong H II 109 $\alpha$  source. At this longitude we are probably encountering the outer regions of the Sagittarius Arm. We conclude then from the radio H II 109 $\alpha$  data that the Carina Spiral Feature is confined between  $l^{\text{II}} = 282^\circ$  and  $295^\circ$ , with only extremely distant H II sources ( $d > 10 \text{ kpc}$ ) located between  $l^{\text{II}} = 295^\circ$  and  $305^\circ$ . At  $l^{\text{II}} = 305^\circ$  we encounter the next inner arm. Figure 5 is a basic diagram and will be used to discuss the distribution of young clusters, optical H II regions and cosmic dust.

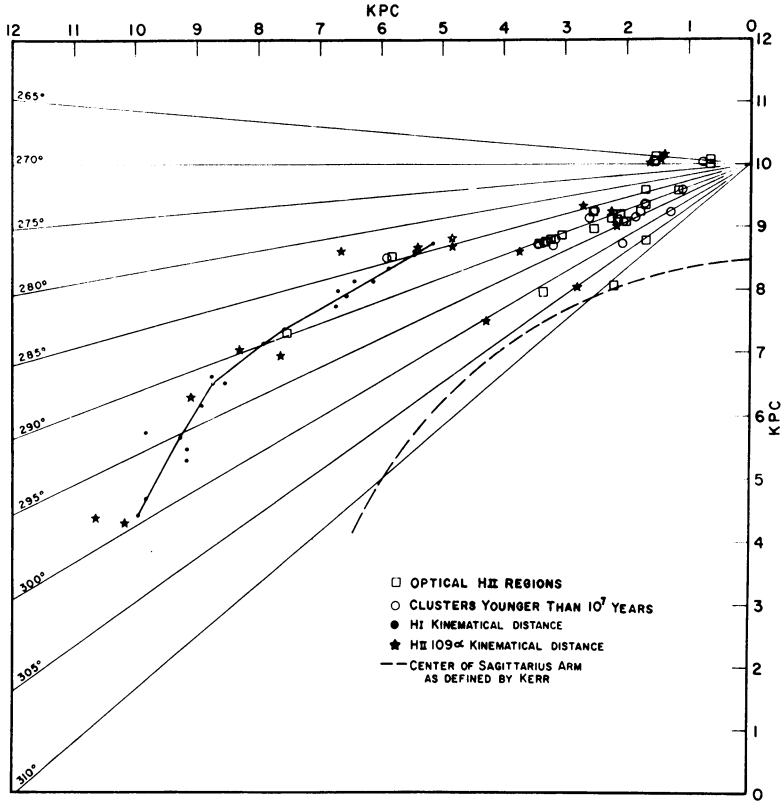


Fig. 6. Young clusters and optical H II regions in Carina. The H II distances indicated by the squares in Figure 6 come principally from Sher's (1965) paper. A few additional H II distances come from Courtès *et al.* (1968). The distances plotted are those of the exciting stars. One H II source, RCW 54 (1), at  $l^{II} = 289^{\circ}.8$ ,  $b^{II} = -1^{\circ}.2$  has been plotted at a distance of 7.9 kpc, Lindsey Smith's (1966) assigned distance for the exciting star. The star is a Wolf-Rayet, WN8, with an OB companion and appears in her list as LS 30. The distance is not unreasonable, as Wilson (1969) finds an H II 109 $\alpha$  source at the same position as the Lindsey Smith H II source at a distance of 9 kpc. Two distant optical H II regions ( $> 5$  kpc) fall along the spiral feature as defined by the H I. These H II regions are Wd 1 (Westerlund, 1960) at 6 kpc and the Lindsey Smith 7.9 kpc region. They support the way in which we have drawn the more distant part of the arm. The Rodgers *et al.* (1960a) optical H II catalogue lists no H II regions between  $l^{II} = 270^{\circ}$  and  $282^{\circ}$ . The radio data show that the lack of H II sources between these longitudes is real and not caused by absorption. The most conspicuous optical sources in the RCW catalogue are located between  $l^{II} = 285^{\circ}$  and  $295^{\circ}$  and at distances between 2 and 4 kpc. These H II regions provide a means of defining the Carina Spiral Feature at distances nearer than 5 kpc from the sun. An outer envelope (towards smaller longitudes) can be drawn around the H II regions. This envelope appears to link up with the H I arm near  $l^{II} = 284^{\circ}$  at a distance of 5 kpc from the sun. If we draw the total spiral arm in this manner, then it is clear that the prominent H II regions are on the inside of the Carina Spiral Feature as defined mostly by H I. If the H II regions were to be placed on the outside of the spiral feature, then we would require the gaseous H I arm to suddenly jut inward near  $l^{II} = 284^{\circ}$ , which seems rather unlikely. Additional information, presented later in the present paper, leads to the conclusion that the H II regions are indeed on the inside of the spiral feature. All but three of the young clusters indicated by circles come from Sher's work (1965). The other three clusters have been included from Lindoff's (1968) paper on ages of open clusters. There are some 140 listed clusters between  $l^{II} = 265^{\circ}$  and  $310^{\circ}$ . Many are older than  $10^7$  years, but a number are believed to be young. Data on the young clusters would certainly improve our analysis of the spatial distribution of clusters in Carina. If one draws the near portion of the spiral feature (within 5 kpc of the sun) as the outer envelope of the H II optical and radio sources, then the clusters appear on the inside of the Carina Spiral Feature.

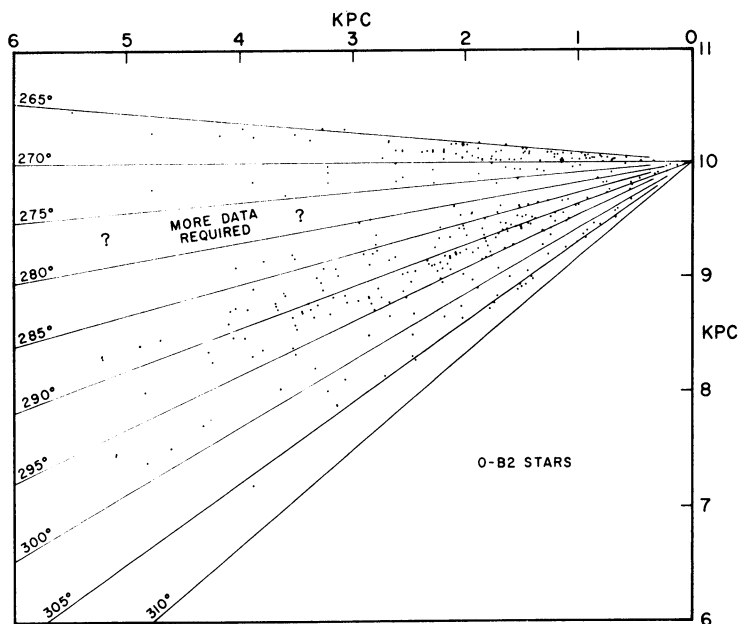


Fig. 7. O-B2 stars. O-B2 stars, which have observed UBV colors, or which have B-V colors and spectral types, are plotted in Figure 7. The distances have been corrected for reddening. All distances from the sun for the stars in this diagram have been placed on a homogeneous basis by using in the reductions the intrinsic colors and absolute magnitudes given by Schmidt-Kaler (1965). For each star the color excess is defined as the difference between the observed (B-V) color and the value of  $(B-V)_0$  of Schmidt-Kaler. The total absorption  $A_V$  is found by multiplying the (B-V) color excess by a factor 3. The absolute magnitudes for the stars in Figure 7 are assigned on the basis of the published luminosity classification. When no luminosity classification exists for the star, the star is assumed to be of class V and the corresponding absolute magnitude for a class V star is then assigned. The stars between  $l^{\text{II}} = 265^\circ$  and  $273^\circ$  are from the unpublished work of Velghe, who kindly made his results available to us in advance of publication. Stars at other longitudes are from the lists given in the references at the end of this paper. The most striking feature in the diagram is the apparent lack of stars between  $l^{\text{II}} = 275^\circ$  and  $285^\circ$ . Bok and Van Wijk (1952) observed the same feature and concluded that the deficiency in early B stars in Vela near  $l^{\text{II}} = 283^\circ$  is real and not due to absorption alone. This region is now being studied by Graham (this volume, p. 262) who has observed stars between  $l^{\text{II}} = 282^\circ$  and  $292^\circ$ , and by Velghe and Denoyelle (this volume, pp. 278 and 281) who are working on O and B stars in Vela. Graham finds from his  $H\beta$  study of 454 OB stars between  $l^{\text{II}} = 282^\circ$  and  $292^\circ$  that the OB stars do not appear at large distances until near  $l^{\text{II}} = 285^\circ$ . At this and greater longitudes he finds OB stars present to great distances along the spiral feature. Figure 7 supports Graham's conclusion in that a large number of O-B2 stars are observed between  $l^{\text{II}} = 285^\circ$  and  $l^{\text{II}} = 295^\circ$ . We would hesitate to draw any definite conclusion from the O-B2 stars plotted in Figure 7 regarding an edge to the spiral feature between  $280^\circ$  and  $285^\circ$  as defined by O-B2 stars. Our sample of stars is too small. However, the Warner and Swasey Observatory (WSO) OB star prism survey is more homogeneous and extends to 12th magnitude. From the (WSO) OB star counts between  $l^{\text{II}} = 265^\circ$  and  $305^\circ$  a sharp peak is found in the star numbers between  $l^{\text{II}} = 285^\circ$  and  $290^\circ$  indicating that the stellar arm begins somewhere between these longitudes. Figure 7 shows a decrease in the numbers of O-B2 stars from  $l^{\text{II}} = 295^\circ$  to  $305^\circ$ . This decrease is also noted in the number of OB stars found between these longitudes in the Warner and Swasey Observatory survey. Absorption might be suggested as a possible cause for the drop in star numbers at  $l^{\text{II}} = 295^\circ$ – $305^\circ$ . However, from the absorption studies we have made between  $l^{\text{II}} = 295^\circ$  and  $305^\circ$  and from studies by Lyngå (1968b) for distant stars between  $l^{\text{II}} = 298^\circ$  and  $306^\circ$ , the absorption is shown to be low in the regions not obviously affected by local obscuration. In agreement with Graham, we conclude from the OB stars that an outer edge to the Carina Spiral Feature is found near  $285^\circ$ , and we find an inner edge occurs near  $l^{\text{II}} = 295^\circ$ .



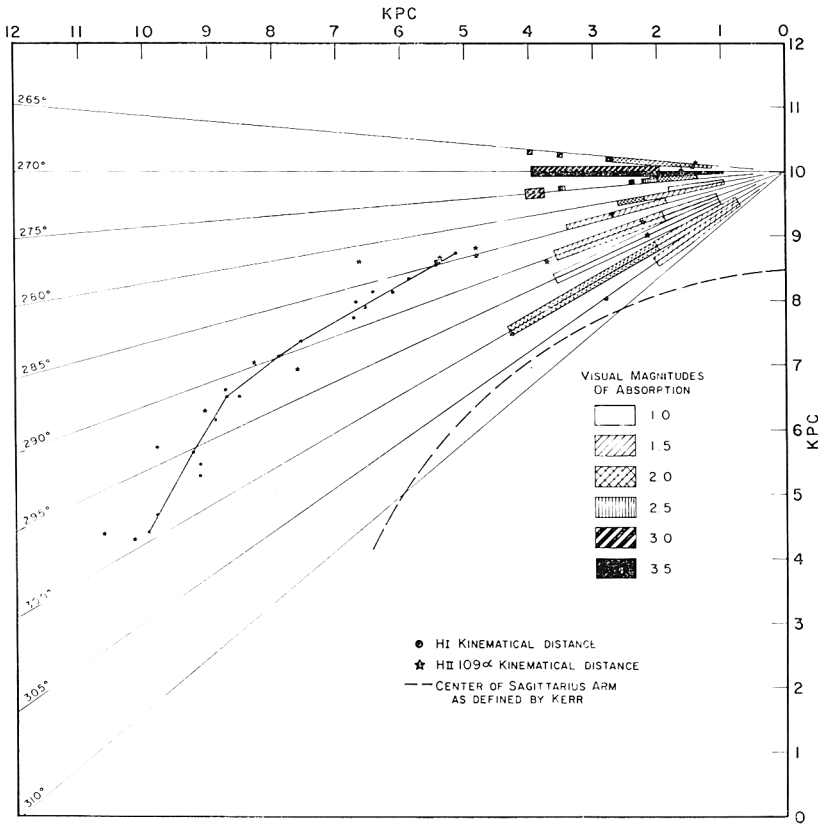


Fig. 8. Absorption in Carina-Centaurus. The magnitudes and colors for the stars that are plotted in Figure 7 form the basis for Figure 8. The only additional data that we have used are the results obtained by Neckel (1967) for the range  $275^\circ < l_{II} < 280^\circ$ , where we have data for only very few stars. High absorption values are found for the range  $265^\circ < l_{II} < 280^\circ$  and generally low values for the range  $282^\circ < l_{II} < 305^\circ$ ; in the latter sector the average visual coefficient of absorption for the areas not obviously affected by local obscuration is  $A_V = 0.5 \text{ mag kpc}^{-1}$ . The low average coefficient of absorption for  $282^\circ < l_{II} < 305^\circ$  renders it possible to penetrate optically to great distances, with stars at distances of 6 to 8 pc becoming accessible to observation. The highest absorption occurs in the range  $265^\circ < l_{II} < 275^\circ$ . Total absorptions in visual light as great as 3 to 4 magnitudes are found in this sector. Our data give information only to a distance of 4 kpc. Without further study we cannot say anything about the total absorptions affecting the stars at greater distances for this critical sector. We take special note of one important structural feature: in the Carina-Centaurus section of the Milky Way, the heaviest absorption is found just on the outside of the Carina Spiral Feature as it is defined by OB stars, clusters and interstellar hydrogen. As of now, this does not appear to be a local phenomenon.

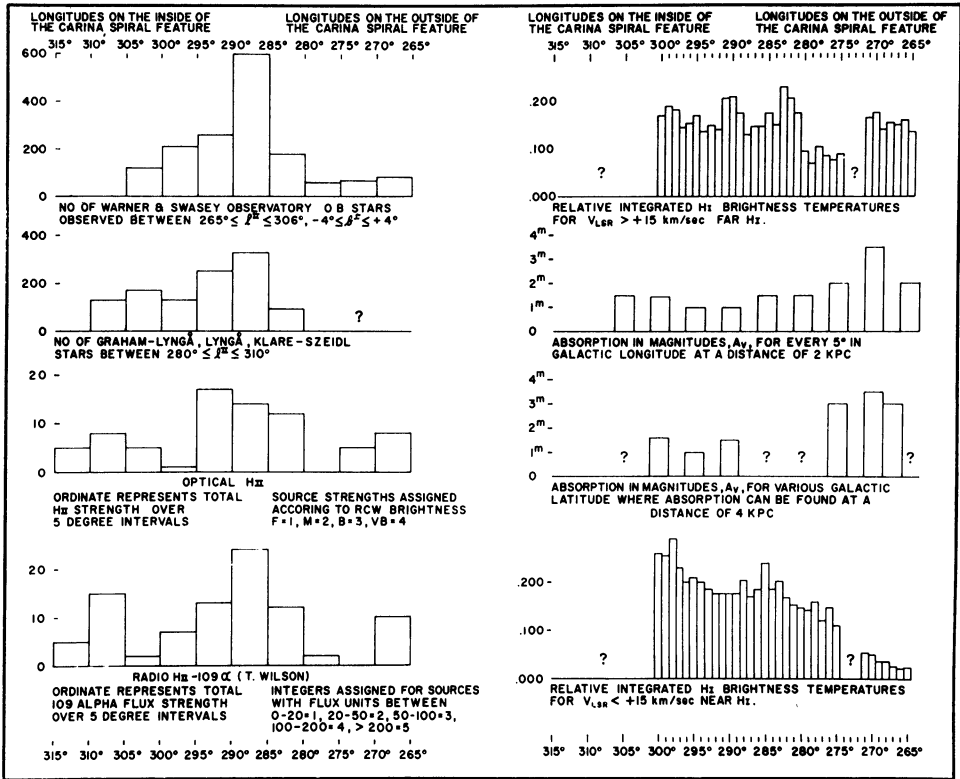


Fig. 9. The distribution of OB stars, optical HII sources, radio HII 109 $\alpha$  sources, H I (far), cosmic dust and H I (near). This diagram collects in a single figure all data obtained thus far. At the top, and on each half of the figure, the galactic longitudes,  $l_{II}$ , are indicated. The question marks indicate areas for which no data are presently available to us. The distribution of OB stars is seen to peak between  $l_{II} = 285^\circ$  and  $290^\circ$  in both the Warner and Swasey Observatory Survey and the combined Graham-Lyngå (1965), Lyngå (1968a), and Klare-Szeidl (1966) OB star searches. Graham has called to our attention the fact that in the Graham-Lyngå OB star search the region near the Carina Nebula was purposely omitted and that, if it had been included, the number of OB stars between  $285^\circ$  and  $290^\circ$  would have been substantially greater than appears in the figure. Warner and Swasey Observatory observations of OB stars for  $l_{II} > 305^\circ$  are available, but they are not included in this progress report. Lyngå has also published OB star data for  $l_{II} > 311^\circ$  (Lyngå, 1964) which we have not used as the data are beyond the galactic longitude limits of our Carina-Centaurus program. The optical HII distribution was determined by assigning to the Rodgers *et al.* (1960a) HII objects source strengths of 1, 2, 3, and 4 depending on their RCW assigned brightnesses. The faintest sources were assigned source strengths of 1, and the very bright HII sources were assigned a value of 4. The ordinate is the sum of the source strengths over  $5^\circ$  intervals of galactic longitude. The peak is seen to occur between longitudes  $290^\circ$  and  $295^\circ$ . The peak between  $290^\circ$  and  $295^\circ$  in the optical HII histogram must be judged with some care, since some faint sources may be distant. If they were close to us, they would be listed as brighter by RCW; the total source strength in  $5^\circ$  longitude intervals might be affected and hence the position of the peak. The Carina Nebula was assigned a source strength of only 4. It could easily be assigned a strength of 40, which would cause the optical HII to peak in the range  $285^\circ$ – $290^\circ$ . The important point is that there is a peak in the optical HII distribution between  $l_{II} = 285^\circ$  and  $295^\circ$  and that it agrees with the OB star peak distribution as shown in the first two diagrams of Figure 9. The distribution of HII 109 $\alpha$  sources studied by Wilson (1969) is shown in the last diagram on the left side of Figure 9. Again source strengths were assigned on the basis of Wilson's published fluxes. 0–20 flux units (f.u.) were assigned a source strength of 1, 20–50 f.u. were assigned a source strength of 2, 50–100

f.u. a strength of 3, 100–200 f.u. a strength of 4 and greater than 200 f.u. a source strength of 5. The source strengths were again summed over  $5^\circ$  intervals and plotted as shown in the histogram. The peak is seen to occur between  $l^{II} = 285^\circ$  and  $290^\circ$ . Some very distant sources will obviously be included with the nearer ones, and there is bound to be an effect in this histogram of the curvature of the spiral feature (see Figures 5 and 6) at distances greater than 9 kpc. A comparison of the histogram for the optical H II sources and that for the radio H II 109 $\alpha$  sources in Figure 9 shows the two distributions peaking at different longitudes. The discrepancy is not of great importance, since the distributions are based on surface brightness or flux without any distance (size) considerations. The peak in the H II 109 $\alpha$  distribution between  $l^{II} = 285^\circ$  and  $290^\circ$  is primarily due to the Carina Nebula, which has a large H II 109 $\alpha$  flux. The important conclusions to be drawn from the H II histograms are that the emission nebulae reach a peak between  $l^{II} = 285^\circ$  and  $295^\circ$  and that on either side of this longitude interval the distribution drops sharply. Between  $l^{II} = 305^\circ$  and  $310^\circ$  the H II sources begin to increase in strength and number, which may indicate a spiral feature closer to the galactic center. The right side of Figure 9 presents the distribution of H I (far and near) and the distribution of absorbing material at distances of 2 and 4 kpc. The neutral hydrogen profiles which we obtained from Kerr and Hindman (1969) are all for positions close to  $b^{II} = 0$ . These profiles were simply integrated by means of a planimeter and the planimeter recordings plotted as a function of longitude. The first plot on the right side of Figure 9 shows the relative integrated H I brightness temperatures for  $V_{LSR}$  (the velocity with respect to the local standard of rest) greater than  $+15 \text{ km s}^{-1}$ ,  $\int_{15}^{\infty} T_b dv$ . The value of  $+15 \text{ km s}^{-1}$  was chosen in order to place the lower limit of the integration well away from any local H I. The velocity profiles reveal a large amount of H I near the solar circle ( $V_{LSR} = 0$ ) between  $l^{II} = 265^\circ$  and  $295^\circ$ , and we wanted to avoid an unnecessary mixing of near and distant H I concentrations.  $V_{LSR} = +15 \text{ km s}^{-1}$  corresponds to a kinematical distance of 5–6 kpc at  $l^{II} = 280^\circ$  for strictly circular velocities; smaller values of  $V_{LSR}$  should refer generally to H I concentrations within 5 kpc, unless marked deviations from circular velocity are present. The striking feature in the diagram is the low integrated  $T_b$  between  $l^{II} = 275^\circ$  and  $280^\circ$ . At  $281^\circ$  the integrated  $T_b$  suddenly increases, as we encounter a large concentration of H I. These large integrated  $T_b$  values continue all the way to the end of our H I data at  $l^{II} = 300^\circ$ . The H I between  $265^\circ$  and  $271^\circ$  is probably local. The radial velocity over these longitudes averages  $+10 \text{ km s}^{-1}$  and corresponds to a kinematical distance of 2 kpc. We consider next the H I integrated  $T_b$  values for  $V_{LSR} < +15 \text{ km s}^{-1}$ . In this histogram we are dealing for the most part with neutral hydrogen which is local, within 3 kpc of the sun. The broadness of the longitude histograms for H I is very striking when a comparison is made with the histograms for the OB stars and for H II. The question marks in the far H I and near H I diagrams are at longitudes where we have no H I profiles. Kerr has velocity profiles for these longitudes, but we have not used them in this progress report. The observed longitude distribution of absorbing material has been plotted for distances of 2 and 4 kpc from the sun. The diagrams refer to average values of the visual absorption,  $A_v$ , for areas within  $3^\circ$  of the galactic equator which are free from easily recognized irregular local obscuration. Both diagrams show a small amount of absorption in Carina between  $l^{II} = 280^\circ$  and  $305^\circ$ . The maximum amount of absorption occurs between  $l^{II} = 265^\circ$  and  $275^\circ$ , where it reaches 3.5 magnitudes at some longitudes.

## 2. Conclusions and Recommendations

### A. CONCLUSIONS

The primary conclusion of the present investigation for the Carina-Centaurus Section between  $l^{II} = 280^\circ$  and  $l^{II} = 305^\circ$  is that we are observing at these longitudes lengthwise along a major Spiral Feature, stretching in distance between 1 kpc and 6 kpc from the sun, and probably beyond.

The OB stars and the H II regions, optical and radio, exhibit a sharply-bounded Feature in the range  $283^\circ$  to  $295^\circ$ . Our results are in full agreement with those presented at this Symposium by Graham, who finds a sharp straight edge at  $l^{II} = 285^\circ$  for the distribution in depth of the OB stars with distances between 3 kpc and 9 kpc

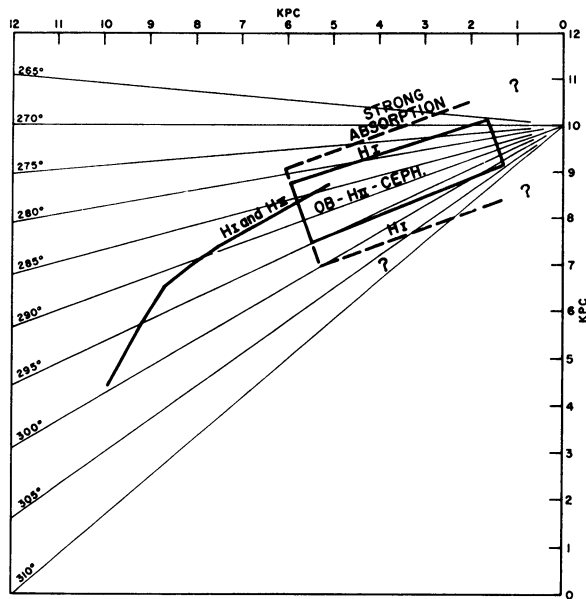


Fig. 10. 1969 working diagram of the Carina spiral feature.

from the sun. Graham finds no super-giant OB stars in the range  $282^\circ < l'' < 285^\circ$ . In a current, as yet unpublished, survey of the distribution in longitude of emission-line stars, Wray and Wackerling find that their distribution exhibits a peak for  $285^\circ < l'' < 295^\circ$ . The H II regions mimic the principal features of the distributions in longitude of the OB stars – as is to be expected – but the neutral hydrogen spills over on both sides of the limited longitude range of the H II concentrations, especially within 4 kpc of the sun. The classical cepheids, studied by Fernie (1968), exhibit precisely the same pattern as the OB stars; this is shown most clearly by Fernie's Figure 2. The density of absorbing matter increases very markedly on the outside of the edge near  $l'' = 283^\circ$ , with very high values of  $A_V$  found for the range  $265^\circ < l'' < 275^\circ$ .

We have noted above that the Spiral Feature appears to be broader in H I than in H II, in OB stars or in cepheids. A 1969 working diagram of the Carina Spiral Feature is shown in Figure 10. At a distance of 4 kpc from the sun, the OB and H II peaks in the longitude distribution are about  $12^\circ$  in width, which implies a linear width of the spiral feature of about 800 pcs. The H I feature has about twice the width, 1500 pcs across, more or less. The peak of the H II and OB star distribution is approximately  $8^\circ$  within the outer edge of the spiral feature shown in H I, hence within 600 pcs of the outer boundary of the H I spiral feature.

We note further that the Spiral Feature in Carina lies surprisingly far below the traditional galactic circle. OB stars and H II regions are found in greatest concentration in the range  $-2^\circ < b'' < 0^\circ$ . Kerr (1969a) has found that the greatest H I concentration in Carina is well below the plane, near  $b'' = -1^\circ$  to  $-1.5^\circ$  for  $l'' = 265^\circ$  to  $310^\circ$ . Unfortunately the data available to us for the H I profiles near  $b'' = -1.5^\circ$  are very

scanty. The consequences of the peculiar latitude distribution of the spiral tracers are fully discussed in Dr. Graham's paper (this volume, p. 262).

The general absorption in Carina-Centaurus is quite small, at least for the regions not obviously affected by local obscuration.  $A_v=0.5 \text{ mag kpc}^{-1}$  is a good average for the range  $280^\circ < l'' < 300^\circ$  and for distances to 4 kpc from the sun. The heaviest absorption is found at  $265^\circ < l'' < 275^\circ$  on the *outside* of our Spiral Feature. Some of the heavy absorption originates within 1 kpc of the sun, but there is good evidence for further heavy absorption setting in at distances between 3 and 4 kpc from the sun. Hence the heavy absorption on the *outside* of the Carina Spiral Feature is not a local phenomenon. However, it is not beyond the realm of possibilities that this heavy concentration of cosmic dust is really at the inside of the next spiral arm, visible in Puppis and Vela! This is a question beyond the scope of our present study.

We refer throughout our Paper to the *Carina Spiral Feature* rather than to the *Carina Spiral Arm*. The Feature that we have described may either be a part of a major spiral arm, or it may represent a very strong link between the Sagittarius and Orion Arms. We shall require studies comparable to ours for several other sections of galactic longitude before we can hope to fit the Carina Spiral Feature into an overall pattern.

## B. RECOMMENDATIONS

In the course of our researches on the Carina Spiral Feature, we have found several gaps in our basic observational data which, if possible, should be filled in the years to come. We list six projects that seem most in need of attention.

### (a) H I Survey

We need most urgently a high resolution 21 cm survey for each degree of longitude in the range  $265^\circ < l'' < 310^\circ$ , with profiles for each degree of latitude between  $b''=0^\circ$  and  $\pm 5^\circ$ .

### (b) A Search for Faint OB Stars

Since adequate UBV sequences are now available to  $V=15$ , we are undertaking the search for OB stars in the range  $12 < V < 15$ , possibly to somewhat fainter limits. The techniques are quite straightforward (Bok, 1966) and simple to apply. Not only will we thus obtain better data on the stellar distribution of young stars in the Carina Spiral Feature, but improved information on interstellar absorption should become available through such studies. We either have, or can readily obtain, the photographic plates required for these studies.

### (c) Open Clusters

There are approximately 140 open clusters listed for the Carina-Centaurus section, of which so far only 20 have been studied in some detail. There are several clusters with probable ages of the order of  $10^7$  years or less that await further study. Distance determinations for young clusters with an associated H II region would assist greatly in the study of the distances of the H II regions.

(d) *Optical Radial Velocities*

With image tubes and other specialized auxiliary apparatus tested and available, it becomes imperative to measure optical radial velocities for a large sample of OB stars and clusters and for all optical H II regions. There is at present little new information available to supplement the fine analysis of stellar and nebular radial velocities carried out some years ago by Feast and Shuttlesworth (1965). Spiral theory demands as much information as is obtainable about differences of velocity between stars and gas. A useful by-product of optical radial velocity data for H II regions will be that these should enable us to list without doubt whether or not a given H II region shown optically is the same as one in the same direction observed by the radio H II 109  $\alpha$ -techniques. High dispersion studies of interstellar absorption lines will obviously be of great importance.

(e) *Polarization*

We have as yet only very incomplete information on the interstellar polarization for the Carina-Centaurus section. The new data by Mathewson, and by Klare and Neckel reported in this volume should prove very helpful but much work remains to be done.

(f) *Long-Period Cepheids*

The Harvard and Leiden variable star surveys have yielded very useful information on the long-period cepheid variables in this section, but the interpretation of the data in relation to spiral structure is confused by the statistical inhomogeneity of the searches made to date. As Kraft (1965) has stressed, the long-period cepheids show great promise as optical spiral tracers for large distances from the sun. Color studies, comparable to those of Olmsted (1966), should be undertaken to check on the interstellar absorption to distances up to 10 kpc from the sun.

The Carina-Centaurus section of the Southern Milky Way is rich and ready for harvest.

### Acknowledgements

We wish to acknowledge advice and assistance received from many individuals and organizations. The financial backing for the Project has come from the National Science Foundation, Grant No. GP-7882. We much appreciate the cooperation received from Dr. V. M. Blanco and the Staff of the Cerro Tololo Interamerican Observatory. Following the Chilean visit from the Boks, Dr. J. A. Graham and Dr. R. E. White rounded out some of the incomplete photoelectric and photographic programs. We should record that we have profited greatly from our continued close collaboration with Dr. Graham.

Several colleagues made new material available to us in advance of publication. We wish in this connection to express our gratitude to the following individual astronomers:

B. F. Burke, W. Buscombe, G. Courtès, T. Denoyelle, A. Feinstein, S. Garzoli, D. Goniadski, J. A. Graham, J. V. Hindman, D. Hoffleit, P. M. Kennedy, F. J. Kerr, G. R. Knapp, S. L. Knapp, C. C. Lin, G. Lyngå, S. W. McCuskey, D. S. Mathewson,

P. G. Mezger, G. Monnet, W. W. Roberts Jr., N. Sanduleak, D. Sher, C. B. Stephenson, C. M. Varsavsky, A. G. Velghe, L. R. Wackerling, G. Westerhout, B. Westerland, T. L. Wilson, J. D. Wray, C. Yuan.

In conclusion we should mention the persons at Steward Observatory who have been deeply involved in the Project, Mrs. Lynn Glaspey, K. Ebisch, D. B. Daer, and E. D. Howell.

### References

- Baade, W. and Mayall, N. U.: 1951, *Problems of Cosmical Aerodynamics* Central Air Documents Office, Dayton, Ohio, p. 165.
- Becker, W.: 1956, *Vistas in Astronomy* **2**, 1515.
- Becker, W.: 1963, *Z. Astrophys.* **57**, 117.
- Becker, W.: 1964, *Z. Astrophys.* **58**, 202.
- Becker, W. and Fenkart, R.: 1963, *Z. Astrophys.* **56**, 257.
- Beer, A.: 1961, *Monthly Notices Roy. Astron. Soc.* **121**, 191.
- Bok, B. J.: 1932, *Harvard Repr.* No. 77.
- Bok, B. J.: 1956, *Vistas in Astronomy* **2**, 1522.
- Bok, B. J.: 1959, *Observatory* **79**, 58.
- Bok, B. J.: 1966, IAU Symposium No. 24, p. 228.
- Bok, B. J. and P. F.: 1960, *Monthly Notices Roy. Astron. Soc.* **121**, 531.
- Bok, B. J. and P. F.: 1969, *Astron. J.* **74**, 1125.
- Bok, B. J. and van Wijk, U.: 1952, *Astron. J.* **57**, 213.
- Courtès, G.: 1969, private communication.
- Courtès, G., Georgelin, Y. P. and Y. M., Monnet, G., and Pourcelot, A.: 1968, in *Interstellar Ionized Hydrogen* (ed. by Y. Terzian), Benjamin, New York, p. 571.
- Cousins, A. W. J. and Stoy, R. H.: 1963, *Roy. Obs. Bull.*, No. 64.
- Ewen, H. I. and Purcell, E. M.: 1951, *Nature* **168**, 356.
- Feast, M. W., Stoy, R. H., Thackeray, A. D., and Wesselink, A. J.: 1961, *Monthly Notices Roy. Astron. Soc.* **122**, 239.
- Feast, M. W. and Shuttleworth, M.: 1965, *Monthly Notices Roy. Astron. Soc.* **130**, 245, and corrigenda **134**, 107.
- Feinstein, A.: 1969, *Monthly Notices Roy. Astron. Soc.* **143**, 273.
- Fernie, J. D.: 1968, *Astron. J.* **73**, 995.
- Graham, J. A.: 1970, IAU Symposium No. 38, p. 262.
- Graham, J. A. and Lyngå, G.: 1965, *Mem. Mt Stromlo Obs.*, No. 18.
- Hill, E. R.: 1968, *Australian J. Phys.* **21**, 735.
- Hindman, J. V.: 1969, in preparation.
- Hoffleit, D.: 1953, *Harvard Ann.* **119**, 37.
- Kerr, F. J.: 1969a, *Ann. Rev. Astron. Astrophys.* **7**, 39.
- Kerr, F. J.: 1969b, *Austr. J. Phys. Astrophys. Suppl.* **9**, 1.
- Kerr, F. J. and Hindman, J. V.: 1969, in preparation.
- Klare, G. and Szeidl, B.: 1966, *Veröff. Landessternwarte Heidelberg-Königstuhl* **18**, 9.
- Kraft, R. R.: 1965, *Stars and Stellar Systems* **5**, 157.
- Lindoff, U.: 1968, *Ark. Astron.* **5**, 1.
- Lodén, L. O.: 1968, *Ark. Astron.* **5**, 161.
- Lyngå, G.: 1964, *Medd. Lund Obs.*, Series II, No. 39.
- Lyngå, G.: 1968a, *Ark. Astron.* **5**, 161.
- Lyngå, G.: 1968b, *Proc. Astron. Soc. Austr.* **1**, 92.
- Mathewson, D. S., Healey, J. R., and Rome, J. M.: 1962, *Austr. J. Phys.* **15**, 354.
- Morgan, W. W., Sharpless, S., and Osterbrock, D. E.: 1952, *Astron. J.* **57**, 3.
- Neckel, T.: 1967, *Veröff. Landessternwarte Heidelberg-Königstuhl* **19**.
- Olmsted, M.: 1966, *Astron. J.* **71**, 916.
- Oort, J. H., Kerr, F. J., and Westerhout, G.: 1958, *Monthly Notices Roy. Astron. Soc.* **118**, 379.
- Rodgers, A. W., Campbell, C. T., and Whiteoak, J. B.: 1960a, *Monthly Notices Roy. Astron. Soc.* **121**, 103.

- Rodgers, A. W., Campbell, C. T., Whiteoak, J. B., Bailey, H. H., and Hunt, V. O.: 1960b, *An Atlas of H-Alpha Emission in the Southern Milky Way*, Mt Stromlo Obs., Australian National Univ., Canberra.
- Schmidt, M.: 1965, *Stars and Stellar Systems* **5**, 513.
- Schmidt-Kaler, T.: 1964, *Z. Astrophys.* **58**, 217.
- Schmidt-Kaler, T.: 1965, *Landolt-Börnstein, New Series* **1**, 284.
- Sher, D.: 1965, *Quart. J. Roy. Astron. Soc.* **6**, 299.
- Smith, L. F.: 1966, Ph. D. Thesis, Australian National University.
- Velghe, A. G.: 1969, unpublished.
- Westerhout, G.: 1968, *Maryland-Green Bank Galactic 21 cm Line Survey*, 2nd ed., Univ. of Maryland.
- Westerlund, B. E.: 1960, *Ark. Astron.* **2**, 419.
- Wilson, T. L.: 1969, Ph.D. Thesis, M.I.T.